Non-invasive Regulation of Cellular Morphology Using a Photoswitchable Mechanical DNA Polymer

Soumya Sethi, [a] Kumi Hidaka, [a] Hiroshi Sugiyama,* [a][b] and Masayuki Endo*[a][b]

[a]   S. Sethi, K. Hidaka, Prof. Dr. H. Sugiyama, Prof. Dr. M. Endo
        Department of Chemistry, Graduate School of Science
        Kyoto University
        Yoshida-ushinomiyacho, Sakyo-ku, Kyoto 606-8501, Japan
        E-mail: endo@kuchem.kyoto-u.ac.jp; hs@kuchem.kyoto-u.ac.jp
[b]   Prof. Dr. M. Endo, Prof. Dr. Sugiyama
        Institute for Integrated Cell-Material Sciences
        Kyoto University

        Supporting information for this article is given via a link at the end of the document.

Abstract: The extracellular matrix, residing the cells provides a dynamic and reversible environment to the cells. These spatial and temporal cues are essential for the cells especially when they are undergoing morphogenesis, repair, and differentiation. Recapitulation of such an intricate system with reversible presentation of nanoscale cues can help us better understand important cellular processes and can allow us to precisely manipulate cell function in vitro. Herein, we formulated a photoswitchable DNA mechanical nanostructure containing azobenzene moieties, and dynamically regulated the spatial distance between adhesion peptides using the photoswitchable mechanical DNA polymer with photoirradiation. We found that the DNA polymer reversibly forms two different structures, a relaxed linear and shrinked compact form, which were observed by AFM. Using the mechanical properties of this DNA polymer, UV and visible light irradiation induced a significant morphology change of the cells between a round shape and spindle-like shape, which thus provides us a tool to decipher the language of the extracellular matrix better. This study presents a general strategy to explore nanoscale interactions between stem cells and stimuli responsive mechanical DNA nanostructures.

Introduction

Cells in their native microenvironment receive signals dynamically, reversibly and synergistically. The extracellular environment that surrounds the cells has a unique composition and topology and regulates crucial cellular processes like cell adhesion, migration, proliferation and differentiation through a reciprocal and reversible dialogue between various cellular components and receptors.[1],[2]   To artificially mimic the extracellular environment, it is imperative to emulate the nanoscale precision of the native microenvironment along with the dynamic and reversible nature of the matrix. Current existing techniques mostly provide static cell adhesions[3] or non-reversible dynamic substrates.[4],[5]

DNA is considered as an ideal candidate to form highly programmable nanostructures due to its property of sequence-specific hybridization.[6] Previous reports have shown that DNA can form extracellular matrix (ECM) like scaffolds effectively for instance DNA nanoribbons decorated with cell adhesion peptides,[7] nanotubes labelled with cell binding peptides,[8] DNA origami nanoarrays,[9] nanocalipers,[10] DNA based hydrogels[11] etc. which have been shown to support cell adhesion, growth, proliferation and differentiation. These systems mimic nanoscale cues provided for the cells but lack in providing a dynamic and reversible environment with a spatio-temporal control. Recent reports display the use of strand displacement controlled DNA nanomachines[12],[13] to effect the cellular morphology. Such DNA nanomachines involve DNA hybridization reactions, which tend to consume molecular fuels for each cycle and thereby leading to accumulation of unwanted molecular waste in the reaction mixture, providing only a temporal control and thus, limiting the reversibility and efficiency of the system.

Controlling the changes by employing external stimuli like photoirradiation can help overcome the challenges faced by the pre-existing methods. Photocontrol can add another dimension of control to the existing system i.e. a spatial control.   A photoresponsive DNA coupled with azobenzene moieties has been reported to reversibly control hybridization and dehybridization of the DNA strands caused by switching between the cis/trans state of azobenzene with photoirradiation.[14] Using this system as a principle of design, photocontrolled DNA nanodevices were constructed for biological applications.[15],[16],[17]

In this study, we designed a photoresponsive mechanical DNA polymer that can dynamically and reversibly cause a displacement of the cell adhesion peptides (RGD) (Figure 1). The photoresponsive DNA polymer with azobenzene photoswitches were designed to reversibly form a relaxed linear and shrinked compact structure depending on the photoirradiation wavelengths. Using this DNA polymer as an ECM, we reversibly regulate the morphology change of the cells from a spindle shaped morphology with few stress fibres to a rounder morphology with defined stress fibres (Figure 1a). The reversible and dynamic change in the distance of the adhesion peptides in the DNA polymer should significantly affect the morphology of the cells and consequent induction of cellular responses, and thus help us provide a spatial and temporal control over the cellular morphology.
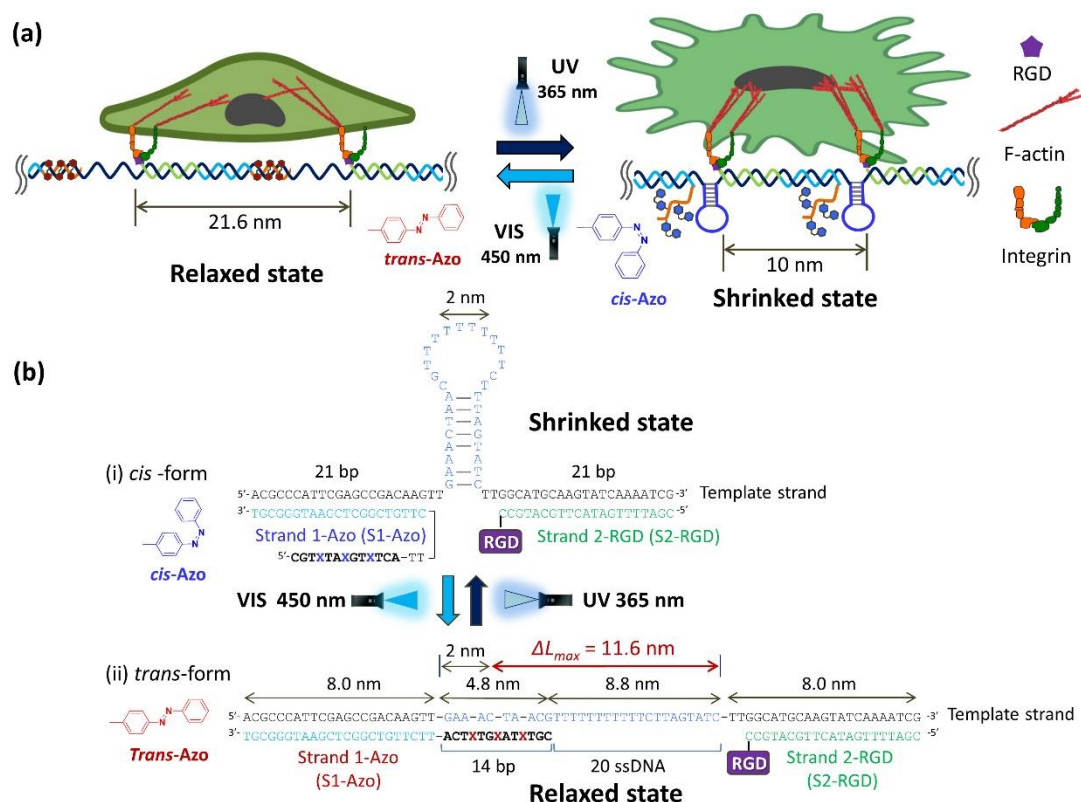
Results and Discussion

Figure 1. Photoresponsive mechanical DNA polymer for spatial and temporal control of cellular morphology. (a) Schematic diagram of the photoresponsive mechanical DNA polymer depicts the cell morphology change as the conformation of the DNA polymer changes. (b) Design of the DNA component and the predicted conformation and distance change when the DNA component is subjected to UV- VIS irradiation. (i) Hairpin formation is predicted when azobenzenes incorporated in strand 1 (S1-Azo) are in cis conformation. (ii) Disruption of the hairpin and hybridization of S1-Azo (trans-form) upon VIS irradiation.

Design of the photocontrolled mechanical DNA polymer

We designed a DNA component structure to control the distance between the cell adhesion peptides, which was inspired by a previous report. [12] We introduced azobenzene moieties in one DNA strand labelled as Strand1-Azo (S1-Azo). To perform photocontrolled conformational change of the component, the DNA component forms a linear structure under visible light, where the azobenzene moieties take the *trans* conformation for hybridization, whereas under UV light the azobenzene moieties take the *cis* conformation for dehybridization and consequently the hairpin formation occurs in the template strand (Figure 1b). The DNA component structure was also designed to cause a reversible change in the conformation by photoirradiation. This conformational change of the DNA component can induce 11.6 nm expansion and shirinking in length between the two states.

Studying the shrinking and relaxation of the photocontrolled mechanical DNA structure

To characterize the conformational change of the photoresponsive DNA component, we performed the gel electrophoresis and AFM observation. The conformational change was detected by the shift of the bands in the native PAGE gel (Figure 2a). The initial structure was formed with S1-Azo (*trans*-form), S2, and complementary strand by annealing, and migrated as a single band in the gel (lane 3). Next, we used UV irradiation (365 nm, 37°C for 10 min) to induce conformational change of the structure. Interestingly, after UV irradiation, the bands of the formed structure appeared multiple and migrated slower (lane 4), indicating that the DNA component with *cis*-

azobenzenes tended to interact each other and formed multiple structures. DNA assembly formed using UV irradiated S1-Azo (*cis*-form) also showed the same pattern of migration bands in the gel (lane 2). The single-stranded *cis*-azobenzene strand in S1-Azo may interact with single-stranded hairpin loop part of another component, thus the existence of the lower mobility bands in the UV irradiated samples. After VIS irradiation (450 nm, 37°C for 10 min), the lower mobility bands completely disappeared and returned to the initial band (lane 5). Although the conformation of the DNA component in *cis*-form is unclear, the reversibility of the conformations of the DNA component and the interaction can be controlled by switching of photoisomerization of azobenzene moieties with UV and VIS irradiation.

Next, to further characterize the conformational change in solution, we used a FAM/Dabcyl fluorescence quenching system (Figure S2). The template strand (76-nt) was consecutively hybridized with an FAM-labelled Strand 2 (F-S2, fluorophore) and a UV irradiated (37°C for 10 min) dabcyl-labelled Strand 1-Azo (Q-S1-Azo, quencher). This annealed product was then UV irradiated (37°C for 10 min). After UV irradiation, the fluorescence intensity decreased by 14%, showing that the quenching occurred by approaching the FAM and quencher in the shrinked state. The quenching efficiency was not strong enough maybe because the position to introduce the quencher was fixed in the internal strand and was not optimized. After VIS irradiation (37°C for 10 min), the fluorescence intensity recovered, indicating that the conformation returned to the relaxed state. Moreover, this DNA component could continuously cycle between the two states, cyclic conversion of the two states is depicted in Figure S2, and it is
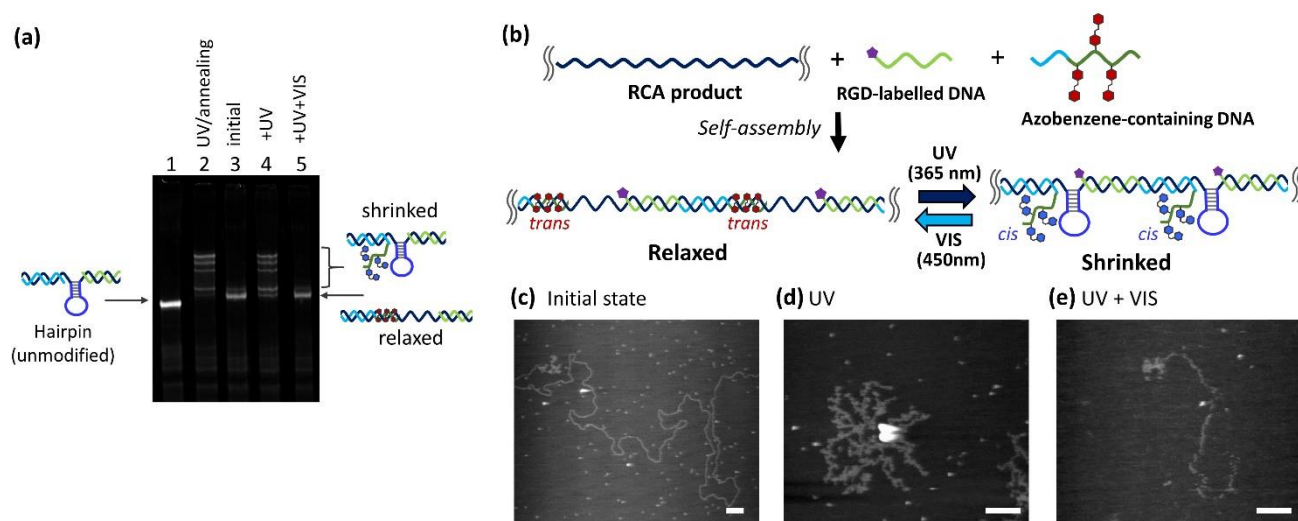
Figure 2. Reversible conformational change of Azo-containing DNA component induced by the photoisomerization with UV/VIS irradiation. (a) Photocontrol mechanical switching of the DNA component structure with UV-VIS irradiation. 15%-native PAGE gel was used for the characterization of the conformation of the DNA component upon UV and VIS irradiation. (b) A long DNA sequence generated using rolling circle amplification (RCA) was used as a template to assemble the photoresponsive DNA strand (S1-Azo) and RGD-labelled strand (S2-RGD). (c) AFM image of initial state of the DNA polymer after annealing with RCA product, S1-Azo and S2-RGD. (d) AFM image of DNA polymer after UV irradiation. (e) AFM image of DNA polymer after sequential UV and VIS irradiation. Scale bar: 100 nm

shown that the component structure could continuously cycle between the linear and hairpin states. Although the signal strength reduction seems lower than expected, we could obtain distinct and reversible migration on the gel, showing that our DNA component could be employed for the further polymerization to prepare a photoresponsive mechanical DNA polymer.

Reversibility of the photocontrolled mechanical DNA polymer

We next prepared a photoresponsive DNA polymer using a long scaffold strand prepared by rolling circle amplification (RCA) (Figure 2b). The size of the RCA product was estimated to be around 15,000 bp from the gel and the AFM images (Figure S1). The long scaffold was annealed with the complementary strands (S1-Azo and S2) at 85 °C to 15°C at a rate of -1.0 °C /min in a buffer containing 20 mM Tris-HCl (pH 7.6), 5 mM MgCl$_2$ and 50 mM NaCl. The molar ratio of RCA product and S1-Azo was 1:200 to study the contraction and relaxation in an amber coloured tube to protect the azobenzene strand from light.

The sample was divided into three parts; Sample 1 – relaxed state whereby observations were made immediately after annealing the mixture; Sample 2 – shrinked state whereby UV was irradiated at 37°C for 10 min; Sample 3 – re-relaxed state whereby UV, followed by VIS was irradiated at 37°C for 10 min. All the samples were observed using high-speed AFM (Figure 2c-e). Figure 2c represents AFM image of the initial state of the DNA polymer after assembling. We observed a long linear structure with flexibility. Then after UV-irradiation, the DNA polymer was observed as a shrinked nanostructure (Figure 2d), which also contained confined hairpin-like structures in the polymer strand (Figure S3). Interestingly, the shrinked structure seems more compact than expected, suggesting that the azobenzene-containing DNA strands interacted weakly to form a two-dimensional structure. Such an interaction was also observed in migration bands of the DNA component in the native PAGE gel (Figure 2a). As observed here, there was a clear demarcation in the conformations of the relaxed and shrinked nanostructures. Then after VIS irradiation, the DNA polymer reverted back to a

linear structure (Figure 2e). These results indicate that the extension and shrinking of the DNA polymer occurred clearly by UV and VIS irradiation. Since UV irradiation induced a formation of a compact structure, we predict this occurrence is due to the interactions of the azobenzene-containing strands that leads to a formation of a compact mesh-like structure. This photoresponsive mechanical DNA polymer was further used for the regulation of cellular morphology.

Photocontrolled mechanical DNA polymer with multivalent cell binding peptides

To facilitate cell binding and spreading onto the formulated mechanical DNA polymer, it was then hybridized to RGD [Cyclo(-RGDfK)] conjugated Strand 2 (S2-RGD). RGD is the peptide sequence known to be a part of the cell binding domain of fibronectin[18] and is shown to have an effective cell binding activity through integrin receptors in many biomaterials.[7],[8] The peptide was conjugated to the DNA using a heterobifunctional linker sulfo-SMCC and subsequently the peptide conjugated DNA was purified using HPLC and characterised on a 20% denaturing page gel (Figure S1c). We next set out to investigate the presence of the RGD onto the DNA polymer, and the adhesion of HeLa cell line was studied on the relaxed DNA polymer coated surfaces. The molar ratio of RCA product: RGD was kept as 1:50. HeLa was chosen as the test cell line because of its highly adherent capabilities. As a negative control, only RCA product-coated surfaces were chosen and as a positive control HeLa cells plated on a cell culture dish (regular cell attachment as control) was chosen. After, the attachment and spreading of the cells, the cells were then fixed and stained with an F-actin stain and a nucleus stain and visualized under a confocal microscope. The area occupied by the cells was analyzed using Image J when seeded on each of the substrates. As shown in the Figure S4, the cells readily adhered on all the three substrates but the cell spreading was evidently more in case of RCA product/S2-RGD (1:50) when compared with only RCA product coated surface. This observation suggests that S2-RGD was successfully hybridized

3

FULL PAPER

to the RCA product and that the presence of RGD on the DNA polymer allowed cells to spread and adhere well.
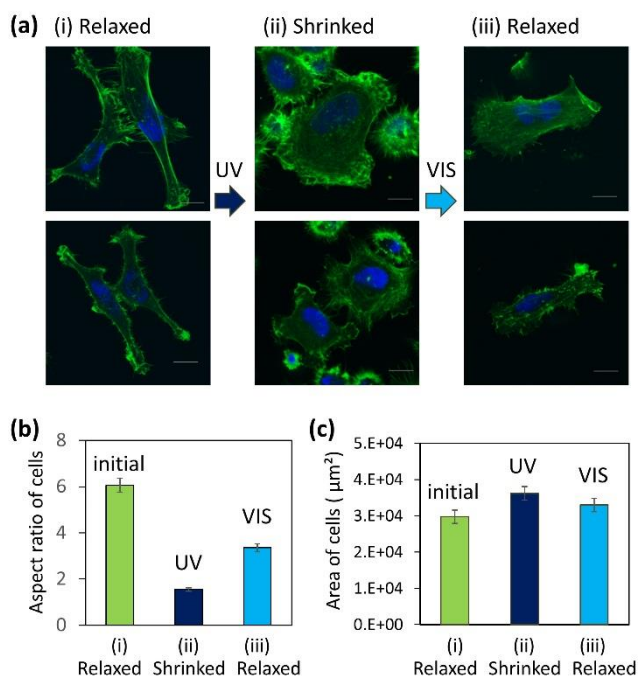

Figure 3. Spatial and Temporal photocontrol of HeLa cell morphology. Photocontrol mechanical switching of DNA Polymer to regulate cell morphology. (a) Representative images of HeLa cells cultured on three different states of the DNA polymer (relaxed, shrinked, re-relaxed) after 9 h of cell culture. Cell nuclei are stained in blue (DAPI staining) and F-actin is stained in green (FITC-labelled phalloidin staining). Scale bar: 10 µm. (b)(c) Aspect ratio of cells and area occupied by the cultured cell on the three substrates were measured and calculated using Image J. 50 cells were analysed for each sample. Error bars (SD) are based on three independent experiments.

Reversible control of HeLa cell morphology using the photoresponsive mechanical DNA polymer

We next investigated the effect of the shrinking and relaxation of the photoresponsive mechanical DNA polymer on HeLa cells. A previous report showed that the morphology of HeLa cells could be regulated using the DNA nanostructure, [12] in which the DNA nanostructure uses DNA hybridization reaction to cause extension and contraction. However, the strand displacement reaction requires the addition of fuel strands each time to induce the conformational changes, which can only be achieved by changing the media, thus not only does it limit repeatability but also can compromise with sterility. Furthermore, although the existing system provides us useful insights in the cell membrane receptor functionality, lags in a spatio-temporal control over the cellular morphology thus limits in emulating the dynamics of the extracellular matrix.

Using our photoresponsive mechanical DNA polymer, we aim to formulate a biomaterial which can provide a spatial and temporal control over the cellular morphology using photo-irradiation. Wavelengths of 365 nm and 450 nm have been reported to cause no harm to cells when used in a controlled intensity and for a controlled time, [19] irradiation can be provided to the cells over the culture plate to the designed area, thus with no compromise in sterility and almost no loss in repeatability can be achieved.

To confirm our hypothesis, we used HeLa cells for the initial experiments. Based on our previous results, the length of the RCA scaffold could be estimated to 200 repeat units, thus, the molar ratios of RCA scaffold: S1-Azo was 1:200 and molar ratio of RCA scaffold: S2-RGD was 1:50 to cause a significant amount of change in the cell morphology when the conformation of the DNA polymer changed. It is imperative to understand that the changes in distances might vary from as shown in Figure 1a in each cycle, as the polymer is a highly flexible DNA scaffold, but we hypothesize from the previous reports[12] that these changes should be good enough to cause a change in the cell morphology. HeLa cells were seeded on the DNA polymer-coated substrates, where all the substrates were initially coated by the relaxed DNA polymer (Figure 3 and S4). After 3h of seeding, the specific areas were irradiated by UV light (10 min at 37°C) to cause shrinking and tension of the DNA polymer. After next 3 h, the specific areas were irradiated by VIS light (10 min at 37°C) to cause re-relaxation of the DNA polymer. A clear difference in the cellular morphology was observed on the cells cultured on the relaxed DNA polymer, where the HeLa cells appear to be well aligned and long in shape (Figure 3a(i) and S5), whereas after UV irradiation, the cells appear to be less aligned, rounder in appearance and better spread (Figure 3a(ii) and S5), so the changes in spreading of the cells were very significant. Further, it was seen that upon irradiation of VIS light the cell morphology reversed back to the relaxed morphology (Figure 3a(iii) and S5). The changes in the morphology were characterized by aspect ratio of cells and area (Figure 3b and 3c), which show that the shrinking and expansion of the cells occurred reversibly upon photoirradiation. Thus, changing the distance between the RGD peptides in the DNA polymer led to a reversible change in the cell morphology, including cell spreading and actin remodelling.

Reversible control of human Mesenchymal Stem Cell morphology using the photo-responsive mechanical DNA polymer

After observing the reversible effects of shrinking and relaxation of the DNA polymer on our HeLa cell test line, we next set out to investigate its effects on human mesenchymal stem cells (hMSCs). It is well known that mesenchymal stem cells have a tremendous potential for tissue engineering applications and can be differentiated into many lineages, researchers have previously investigated the behaviour of MSCs as influenced by various changes in the extracellular matrix.[20],[21],[22],[23],[24],[25] It was clearly demonstrated by the experiments of Frith et al.[26] that lateral displacement of RGD peptide causes morphology changes in the MSCs, which is further exploited to differentiate the cells. Based on these findings, we considered that a dynamic and reversible system might be able to provide further insights into the understanding of cell morphology changes, cell spreading changes, actin re-modelling, and cell differentiation capabilities.

MSCs were cultured onto the photoresponsive DNA polymer coated surface, which was initially on the relaxed state (Figure S6). Consecutively, the coated surface with MSCs was irradiated with UV light (10 min at 37°C) to achieve the shrinked state and then successively irradiated with VIS light (10 min at 37°C) to form a re-relaxed state (Figure 4 and S7). It was observed that on the relaxed DNA polymer i.e. when the RGD adhesion peptides are spaced farther apart, the cell morphology appears to be spindle shaped and well aligned (Figure 4a(i)). After UV irradiation, the cell morphology appears to be more well spread and rounder

because the RGD peptides in the shrinked DNA polymer were relatively close together (Figure 4a(ii)). We also observed significant differences in the organization of actin cytoskeleton. The relaxed state comprised of cells with a disorganized actin cytoskeleton, while the cells on the shrinked state comprised of larger and very well-defined stress fibers (Figure 4a(ii)). After irradiation with VIS light, we observed that the cell morphology reverted back to that of the relaxed state (Figure 4a(iii)). Some of the cells were still in the well spread state, however, majority of the cells reverted to the spindle shape. The changes in the morphology were examined by the change of aspect ratio of cells and area (Figure 4b and 4c), showing that the shrinking and expansion of the cells occurred reversibly. Thus, we could achieve an on-demand reversible control over the cellular morphology. Photocontrol can allow us to specifically alter the morphology in a designated area and has the potential to allow controlled differentiation of MSCs based on the cell shape into different lineages.[26],[27]
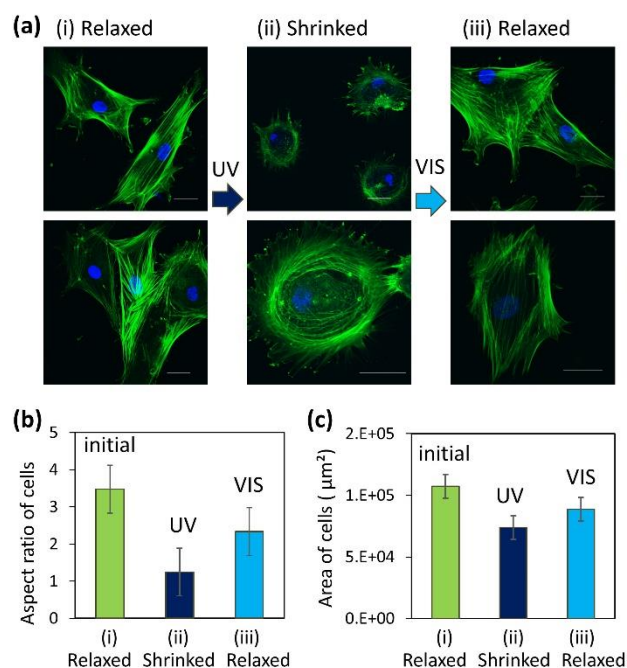

Figure 4. Spatial and Temporal photocontrol of mesenchymal stem cell (MSC) morphology. Photocontrol mechanical switching of DNA polymer to regulate cell morphology. (a) Representative images of MSCs cultured on three different states of the DNA polymer (relaxed, shrinked, re-relaxed state) after 9 h of cell culture. Cell nuclei are stained in blue (DAPI staining) and F-actin is stained in green (FITC-labelled phalloidin staining). Scale bar: 30 µm. (b)(c) Aspect ratio of cells and area occupied by the cultured cell on the three substrates were measured and calculated using Image J. 50 cells were analysed for each sample. Error bars (SD) are based on three independent experiments.

Repeated cycling between the relaxed and shrinked states
We next examined whether our system could undergo the reversible shrinking and relaxation for more than one cycle without any loss in the efficiency. Similar to the previous experiment, we used hMSCs and seeded them onto the DNA polymer coated substrates (relaxed state) and successively irradiated with 2 cycles of UV and VIS and then fixed, stained and observed the cells (Figure 5). We observed a similar cellular morphology changes between the relaxed, shrinked and re-relaxed states (Figure 5a) as we did after only one cycle of

irradiation. The changes in the morphology were similarly observed by the change of aspect ratio of cells and area reversibly (Figure 5b and 5c). Thus, we could conclude that our photoresponsive mechanical DNA polymer caused reversible and dynamic changes in the cellular morphology without any loss in efficiency even with two successive cycles of photoirradiations.
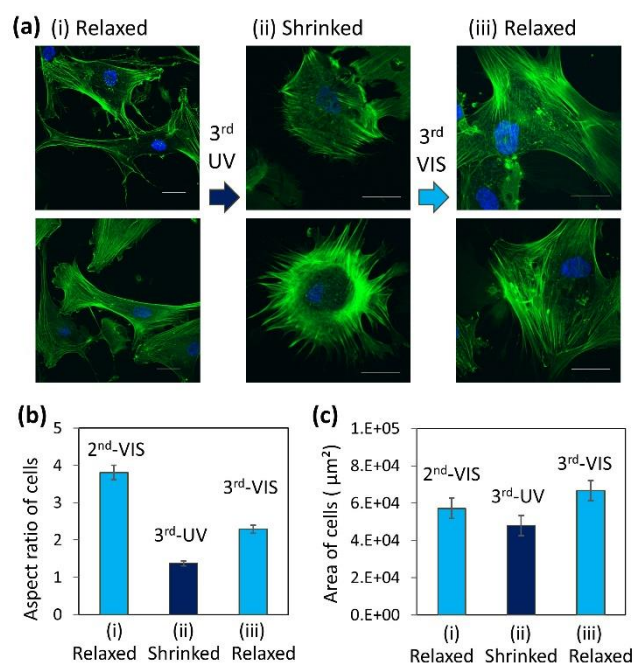

Figure 5. Reversibility of DNA Nanostructure over 2 cycles. Photocontrol mechanical switching of DNA polymer to regulate cell morphology. (a) Representative images of MSCs cultured on three different states of the DNA polymer (second time relaxed, shrinked, re-relaxed) after 18 h of cell culture. Cell nuclei are stained in blue (DAPI staining) and F-actin is stained in green (FITC-labelled phalloidin staining). Scale bar: 30 µm. (b)(c) Aspect ratio of cells and area occupied by the cultured cell on the three substrates were measured and calculated using Image J. 100 cells were analysed for each sample. Error bars (SD) are based on three independent experiments.

Gene Expression evaluation between the shrinked and relaxed states
It is well known that focal adhesion kinase regulates cell adhesion[28],[29] and focal adhesion kinase signalling pathway regulates actin polymerization. Furthermore, it is reported that the clustering of integrins is highly sensitive to the spacing between cell binding ligands and even nanometer distances among ligands can regulate whether or not integrins can form focal adhesion plaques.[30],[31] Thus, we investigated this phenomenon using our photoresponsive mechanical DNA polymer. We performed quantitative polymerase chain reaction (qPCR) of focal adhesion kinase gene, vinculin, and paxillin (Figure 6). Interestingly, our data supports the previously reported results that focal adhesion kinase levels were decreased when MSCs were cultured on larger spaced RGD substrates.[26] We could observe a significant change in relative expression of focal adhesion kinase gene when MSCs were cultured on the shrinked state DNA polymer as opposed to the relaxed state DNA polymer. This also confirms our observations of difference of cell spreading on the relaxed and shrinked DNA polymer. Differences in cell adhesions and spreading causes a significant change in formation of focal adhesions and thus qPCR results support the morphology

changes. Furthermore, vinculin and paxillin are important proteins in focal adhesion complexes,[29] and from our qPCR results we observed a substantial change in the gene expression levels of vinculin and paxillin among the shrinked and relaxed states.
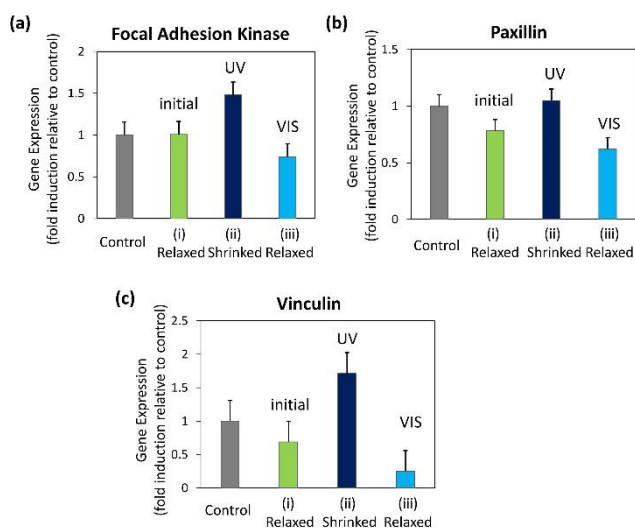

Figure 6. The photoresponsive mechanical DNA polymer to regulate Focal adhesion kinase, Vinculin, Paxillin mRNA expression in MSCs. Focal adhesion kinase (a), Paxillin (b), and Vinculin (c) expression in human MSC cells cultured on four different substrates as indicated. The mRNA expression levels were analysed by RT-qPCR. Gene expressions were normalized using GAPDH. Cell culture plate was chosen as the control substrate. Error bars (SD) are based on three independent experiments.

Conclusion

We have demonstrated that reversible shrinking and relaxation of the designed photoresponsive mechanical DNA polymer with UV and VIS irradiation. Using HeLa and human mesenchymal stem cells, we found that the photoresponsive mechanical DNA polymer labelled with RGD peptide, which causes a displacement of the RGD ligands, in turn causes the change in the spreading of the cell, the organization of the F-actin filaments, and formation of focal adhesions. Our dynamic and photocontrolled reversible DNA polymer can be used as an efficient and effective tool for understanding many important phenomena such as cell morphogenesis, tissue repair, cancer metastasis, cell differentiation etc. All the above-mentioned phenomenon rely on the basis of cell-cell and cell-substrate attachment. Such an extracellular matrix mimicking dynamic tool is very critical and beneficial in understanding and expanding our knowledge.

Acknowledgements

References

[1] C. Frantz, K. M. Stewart, V. M. Weaver, *J. Cell Sci.* **2010**, *123*, 4195–4200.

[2] R. O. Hynes, *Science (80-.).* **2009**, *326*, 1216–1219.

[3] N. Stephanopoulos, J. H. Ortony, S. I. Stupp, *Acta Mater.* **2013**, *61*, 912–930.

[4] S. Sur, J. B. Matson, M. J. Webber, C. J. Newcomb, S. I. Stupp, *ACS Nano* **2012**, *6*, 10776–10785.

[5] S. J. Todd, D. Farrar, J. E. Gough, R. V. Ulijn, *Soft Matter* **2007**, *3*, 547–550.

[6] O. I. Wilner, I. Willner, *Chem. Rev.* **2012**, *112*, 2528–2556.

[7] F. A. Aldaye, W. T. Senapedis, P. A. Silver, J. C. Way, *J. Am. Chem. Soc.* **2010**, *132*, 14727–14729.

[8] N. Stephanopoulos, R. Freeman, H. A. North, S. Sur, S. J. Jeong, F. Tantakitti, J. A. Kessler, S. I. Stupp, *Nano Lett.* **2015**, *15*, 603–609.

[9] D. Huang, K. Patel, S. Perez-Garrido, J. F. Marshall, M. Palma, *ACS Nano* **2019**, *13*, 728–736.

[10] A. Shaw, V. Lundin, E. Petrova, F. Fördos, E. Benson, A. Al-Amin, A. Herland, A. Blokzijl, B. Högberg, A. I. Teixeira, *Nat. Methods* **2014**, *11*, 841–846.

[11] A. Finke, A. K. Schneider, A. S. Spreng, M. Leist, C. M. Niemeyer, A. Marx, *Adv. Healthc. Mater.* **2019**, *8*, 1–7.

[12] K. Zhang, R. Deng, Y. Sun, L. Zhang, J. Li, *Chem. Sci.* **2017**, *8*, 7098–7105.

[13] R. Freeman, N. Stephanopoulos, Z. Álvarez, J. A. Lewis, S. Sur, C. M. Serrano, J. Boekhoven, S. S. Lee, S. I. Stupp, *Nat. Commun.* **2017**, *8*, DOI 10.1038/ncomms15982.

[14] X. Liang, T. Mochizuki, H. Asanuma, *Small* **2009**, *5*, 1761–1768.

[15] M. Zhou, X. Liang, T. Mochizuki, H. Asanuma, *Angew. Chemie - Int. Ed.* **2010**, *49*, 2167–2170.

[16] Q. Yuan, Y. Zhang, T. Chen, D. Lu, Z. Zhao, X. Zhang, Z. Li, C. H. Yan, W. Tan, *ACS Nano* **2012**, *6*, 6337–6344.

[17] G. K. Joshi, K. N. Blodgett, B. B. Muhoberac, M. A. Johnson, K. A. Smith, R. Sardar, *Nano Lett.* **2014**, *14*, 532–540.

[18] M. D. Pierschbacher, E. Ruoslahti, *Nature* **1984**, 3–6.

[19] D. Y. Wong, T. Ranganath, A. M. Kasko, *PLoS One* **2015**, *10*, 1–21.

[20] E. K. F. Yim, E. M. Darling, K. Kulangara, F. Guilak, K. W. Leong, *Biomaterials* **2010**, *31*, 1299–1306.

[21] F. Kantawong, K. E. V. Burgess, K. Jayawardena, A. Hart, R. J. Burchmore, N. Gadegaard, R. O. C. Oreffo, M. J. Dalby, *Biomaterials* **2009**, *30*, 4723–4731.

[22] A. K. Kundu, A. J. Putnam, *Biochem. Biophys. Res. Commun.* **2006**, *347*, 347–357.

[23] A. R. Cameron, J. E. Frith, J. J. Cooper-White, *Biomaterials* **2011**, *32*, 5979–5993.

[24] A. S. Rowlands, P. A. George, J. J. Cooper-White, *Am. J. Physiol. - Cell Physiol.* **2008**, *295*, 1037–1044.

[25] A. J. Engler, S. Sen, H. L. Sweeney, D. E. Discher, *Cell* **2006**, *126*, 677–689.

[26] J. E. Frith, R. J. Mills, J. J. Cooper-White, *J. Cell Sci.* **2012**, *125*, 317–327.

[27] K. A. Kilian, B. Bugarija, B. T. Lahn, M. Mrksich, *PNAS* **2010**, *107*, 4872–4877.

[28] M. S. Bauer, F. Baumann, C. Daday, P. Redondo, E. Durner, M. A. Jobst, L. F. Milles, D. Mercadante, D. A. Pippig, H. E. Gaub, F. Gräter, D. Lietha, *Proc. Natl. Acad. Sci. U. S. A.* **2019**, *116*, 6766–6774.

[29] M. A. Wozniak, K. Modzelewska, L. Kwong, P. J. Keely, *Biochim. Biophys. Acta - Mol. Cell Res.* **2004**, *1692*, 103–119.

[30] M. Arnold, E. A. Cavalcanti-Adam, R. Glass, J. Blümmel, W. Eck, M. Kantlehner, H. Kessler, J. P. Spatz, *ChemPhysChem* **2004**, *5*, 383–388.

[31] E. A. Cavalcanti-Adam, T. Volberg, A. Micoulet, H. Kessler, B. Geiger, J. P. Spatz, *Biophys. J.* **2007**, *92*, 2964–2974.

Entry for the Table of Contents

FULL PAPER

We created a photoswitchable DNA mechanical polymer containing azobenzene moieties, and dynamically regulated the spatial distance between adhesion peptides with photoirradiation. Using the mechanical properties of this DNA polymer, UV and visible light irradiation induced the significant morphology change of the cells between a usual spread state and a shrinked state reversibly. This study presents a general strategy to explore nanoscale interactions between stem cells and stimuli responsive mechanical DNA nanostructures.

Photoswitchable regulation of cellular morphology
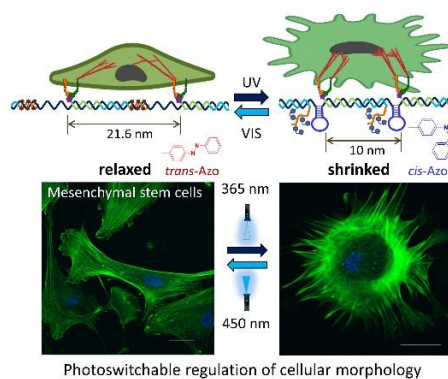
Soumya Sethi, Kumi Hidaka, Hiroshi Sugiyama, and Masayuki Endo**

Non-invasive Regulation of Cellular Morphology Using a Photoswitchable Mechanical DNA Polymer

Supporting Information

Non-invasive Regulation of Cellular Morphology Using a Photo-Responsive Mechanical DNA Polymer

Soumya Sethi, [a] Hidaka Kumi, [a] Hiroshi Sugiyama,* [a][b] and Masayuki Endo*[a][b]

[a] Department of Chemistry, Graduate School of Science, Kyoto University, Kitashirakawa-oiwakecho, Sakyo-ku, Kyoto 606-8502, Japan

[b] Institute for Integrated Cell-Material Sciences, Kyoto University, Yoshida-ushinomiyacho, Sakyo-ku, Kyoto 606-8501, Japan

*To whom the correspondence should be addressed: E-mail: endo@kuchem.kyoto-u.ac.jp, hs@kuchem.kyoto-u.ac.jp

Experimental Section

Materials. All the unmodified oligonucleotides were purchased from Eurofins Genomics (Tokyo, Japan). Azobenzene-containing DNA (Strand 1-Azo) was purchased from Japan Bio Services (Saitama, Japan). The enzymes used for the experiments – Taq DNA ligase, Phi 29 polymerase and dNTPs were purchased from NEB (New England Biolabs, Ipswich, MA, USA). Cyclo-RGD [Cyclo(-RGDfK)] was purchased from ChemScene (Monmouth Junction, NJ, USA). SMCC (sulfosuccinimidyl-4-(*N*-maleimidomethyl)cyclohexane-1-carboxylate) was purchased from ThermoFisher Scientific, TCEP (trichloroethyl phosphate) was purchased from TCI (Tokyo, Japan). FITC labelled phalloidin was purchased from Sigma-Aldrich (St. Louis, MO, USA). FV1200 Laser Scanning Microscope (Olympus) was used for fluorescence imaging. A multimode plate reader (PerkinElmer) was employed for measurement of the fluorescence signal. RT-qPCR study was performed using LightCycler®480 II(Roche). NanoDrop 2000c UV-Vis Spectrophotometer was used for measuring the nucleic acid concentration.

Unit Structure Assembly. The unit structure was assembled using template strand, strand 1-Azo and strand 2 by annealing at 85 °C to 15°C at a rate of -1.0 °C /min in a buffer containing 20 mM Tris HCL (pH 7.6), 5 mM $MgCl_2$ and 50 mM NaCl. For comparison among the conformations, two controls were also assembled, one labelled as control 1 comprising of template strand, strand 1 and strand 2 annealed at 85 °C to 15°C at a rate of -1.0 °C /min and the other labelled as control 2 comprising of template strand, strand 2 annealed at 85 °C to 15°C at a rate of -1.0 °C /min and subsequent mixing of UV irradiated strand 1. To change the conformation of the unit structure, it was subjected to UV irradiation (365 nm at 37 °C) and VIS irradiation (450 nm at 37 °C). The conformations were then characterized using a 15% native PAGE gel.

Photo-irradiation to the unit structure. For the conformation change of the unit structure, UV irradiation was carried out in a microtube at 37°C for 10 min using the Xe-lamp (300 W, Asahi-spectra MAX-303) with a band-path filter (10 nm FWHM) at 365 nm. Then VIS light was irradiated at 37 ° C for 10 min using the Xe-lamp with a band-path filter at 450 nm (14 mW/cm^2). The temperature during the irradiation was controlled using a temperature controlled dry bath.

Ligation of the 76-nucleotide strand. The template strand was subjected to ligation using Taq Ligase enzyme and the reaction was performed at 65°C overnight. After the reaction was complete, the desired ligated product was purified and concentrated and stored for future use.

RCA product synthesis. The elongation of the template strand was done using rolling circle amplification reaction as described previously.[1],[2] We chose various reaction times to optimize the size of the RCA product to be used. Based on the agarose gel electrophoresis characterization, the 10 min product seems to give a uniform product length so we used the 10 min reaction conditions for all the future experiments.

RGD - Strand 2 synthesis. Cyclo-RGD conjugation to the DNA strand 2 was done using a previously described method.[3] The gel shift after conjugation can be seen evidently in Figure S1c.

AFM imaging. The AFM images were obtained using Dimension FastScan (Bruker AXS, Madison, WI) with a silicon nitride cantilever (Olympus BLAC10EGS). Samples were diluted using observation buffer containing 20 mM Tris (pH7.6), 5 mM $MgCl_2$, and 1 mM EDTA. The diluted sample solution (10 µL) was adsorbed onto a mica plate for 5 min at rt and then washed three times using the same observation buffer. Scanning was performed in the same buffer solution using tapping mode.

Preparation and coating of glass slides. Glass slides used for the cell experiments were cleaned thoroughly using sonication in water, ethanol and water each for a duration of 10 min. Subsequently the glass slides were etched by immersing in a piranha solution, following which they were washed with water, ethanol and acetone. After the wash, they were coated with 2% APTES (in acetone) for 3 min and then washed for 3 times in acetone. They were further dried in the oven at 120 °C for 2-3 h and then stored in a sterile environment for future use.

Cell culture. For cell experiments, HeLa cell line purchased from (JCRB Cell Bank Japan) were cultured and maintained in Dulbecco's Modified Eagle Medium (ThermoFisher Scientific) supplemented with 10 % fetal bovine serum (Sigma) and 1% penicillin/streptomycin. Incubation of cell line was done at 37 °C in 5% CO_2 atmosphere with 95% humidity.

Human bone marrow derived mesenchymal stem cells (hMSCs) were purchased RIKEN Cell Bank, Japan and were cultured and maintained in low glucose DMEM (ThermoFisher Scientific) supplemented with 10 % fetal bovine serum (Sigma) and 1% penicillin/ streptomycin. Incubation of cells was done at

37 °C in 5% CO_2 atmosphere with 95% humidity. Cells were used in lower passage number for the experiments.

For the experiment, serum free media supplemented by 1% Insulin-Transferrin-Selenium (ThermoFisher Scientific) was used as we suspect that use of fetal bovine serum might allow non- specific cell adhesions which might interfere in our results.

For the experiment, cells were seeded on 4 substrates (sample 1 on a cell culture dish, sample 2, sample 3, sample 4 on relaxed DNA nanostructure coated glass). The cells were seeded on all the substrates and allowed to adhere and spread for 3 h, next sample 2 and sample 3 were irradiated with UV light (365 nm) for 10 min while incubating the cells at 37 °C. Next, the cells were allowed to spread for 3 hours and the sample 2 was re-irradiated with UV at 365 nm with the same intensity for 10 min while incubating the cells at 37°C so as to maintain the cis conformation of the azobenzene (as the half-life for azobenzene in cis state is considered to be only 3-4 h and sample 3 was irradiated with VIS at 450 nm for 10 min, while incubating the cells at 37°C. After culturing the cells for another 3 hours, the medium was aspirated from the wells and the cells were fixed using 4% paraformaldehyde. No PBS wash was given prior to fixing so as to maintain the actin filament structure. After fixing the cells were washed with PBS 3 times and phase contrast images of each sample were taken.

Similarly, for the 2 cycles, the similar time intervals and procedures were followed and the cells were fixed after 18 h of the experiment and stained and visualised. The cells were then stained with FITC labelled phalloidin and DAPI and then imaged using FV1200 Laser Scanning Microscope (Olympus).

UV- VIS exposure to cells. The UV and VIS irradiation was provided through a LED light source (CL-1501, Asahi Spectra). The LED used for UV irradiation was of the wavelength 365nm (CL-H1-365-9-1, Asahi Spectra) and the intensity of UV light used for the cell experiments was calculated as 16.416 mW/cm^2 keeping into account the working distance and plate dimensions. The LED used for VIS irradiation was of the wavelength 450 nm (CL-H1-450-9-1, Asahi Spectra) and the intensity of light used for the cell experiments was calculated as 14.22 mW/cm^2 keeping into account the working distance and plate dimensions. It should be noted that the reported intensity has been calculated by keeping into account the 8-10% decrease when passed through polystyrene. During the entire time of irradiation, the cells were maintained at 37°C.

Quantitative reverse-transcription PCR analysis (RT-qPCR). After 9h of the experiment, the cells were lysed using a lysis buffer and stored at -80° C until further use. Next, total RNA was extracted from

each sample using FastGene™ RNA Basic Kit (Nippon Genetics) following manufacture's instruction) and reverse transcription was performed from 200 ng of total RNA using ReverTra Ace qPCR RT Kit (Toyobo)according to the manufacturer's instructions. The expression level of the genes (Focal Adhesion Kinase, Paxillin, Viniculin was analyzed by the LightCycler®480 II(Roche)using Thunderbird SYBR q-PCR mix (Toyobo). The mRNA expression level was normalized using GAPDH. The primer sequences are listed in Table S1.
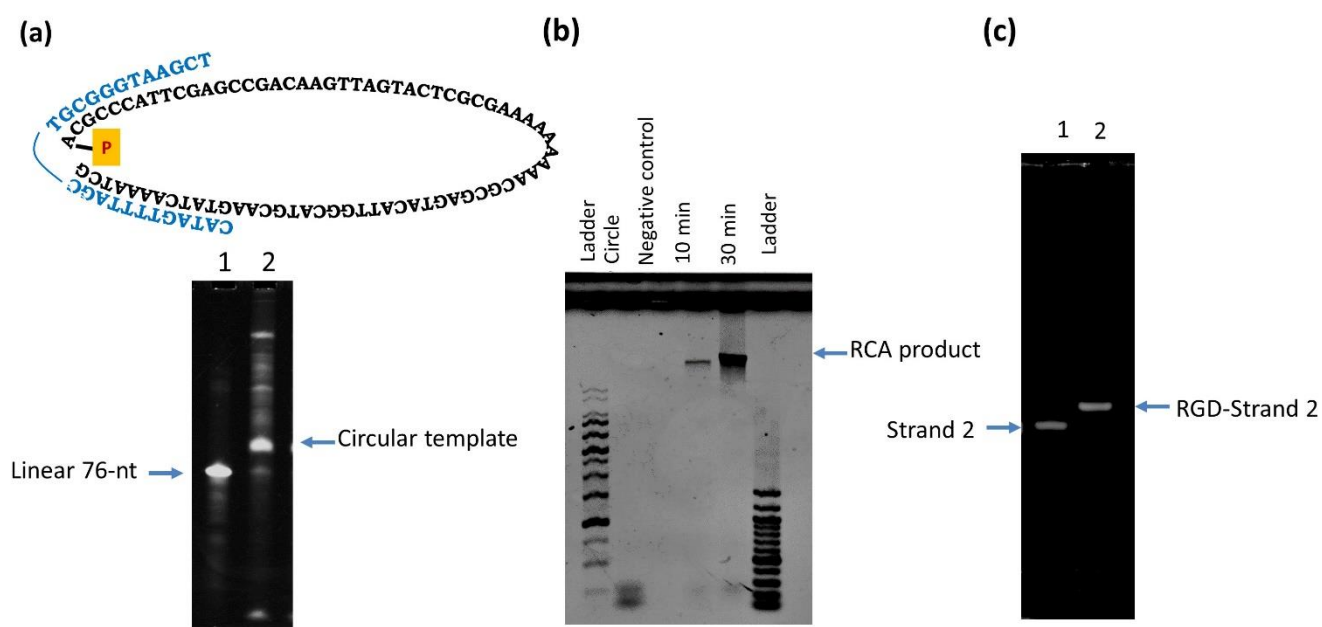

Figure S1. Circular template synthesis and rolling circle amplification (RCA) product characterization. (a) Ligation of the 76-nt template strand, the product was characterized by 8% denaturing PAGE gel and purified from the gel. (b) Characterization of the RCA product. (c) Characterization of the conjugation of RGD to strand-2. HPLC-purified RGD-conjugated strand-2 was analysed by a 20% denaturing PAGE gel (8M urea).
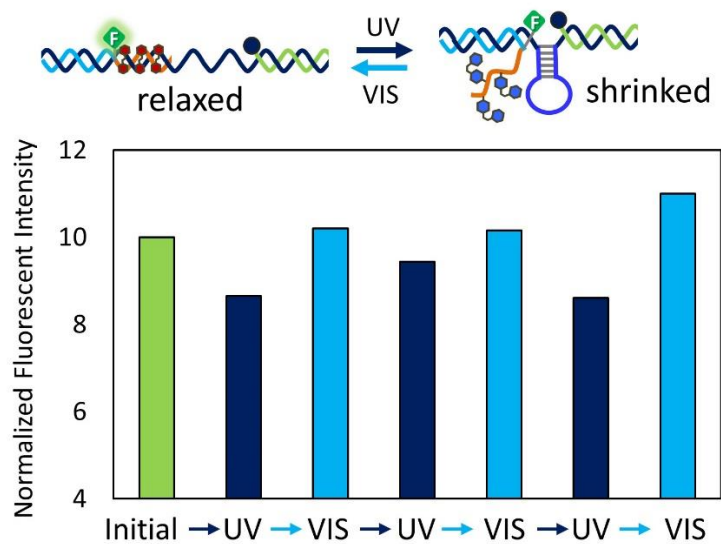
Figure S2. Reversible conformational change of Azo-containing DNA component induced by the photoisomerization with UV/VIS irradiation. Flourescence quenching measurement in the conformational change between relaxed and shrinked states. Cyclic activation of the DNA component between the relaxed and shrinked states by UV and VIS irradiation.
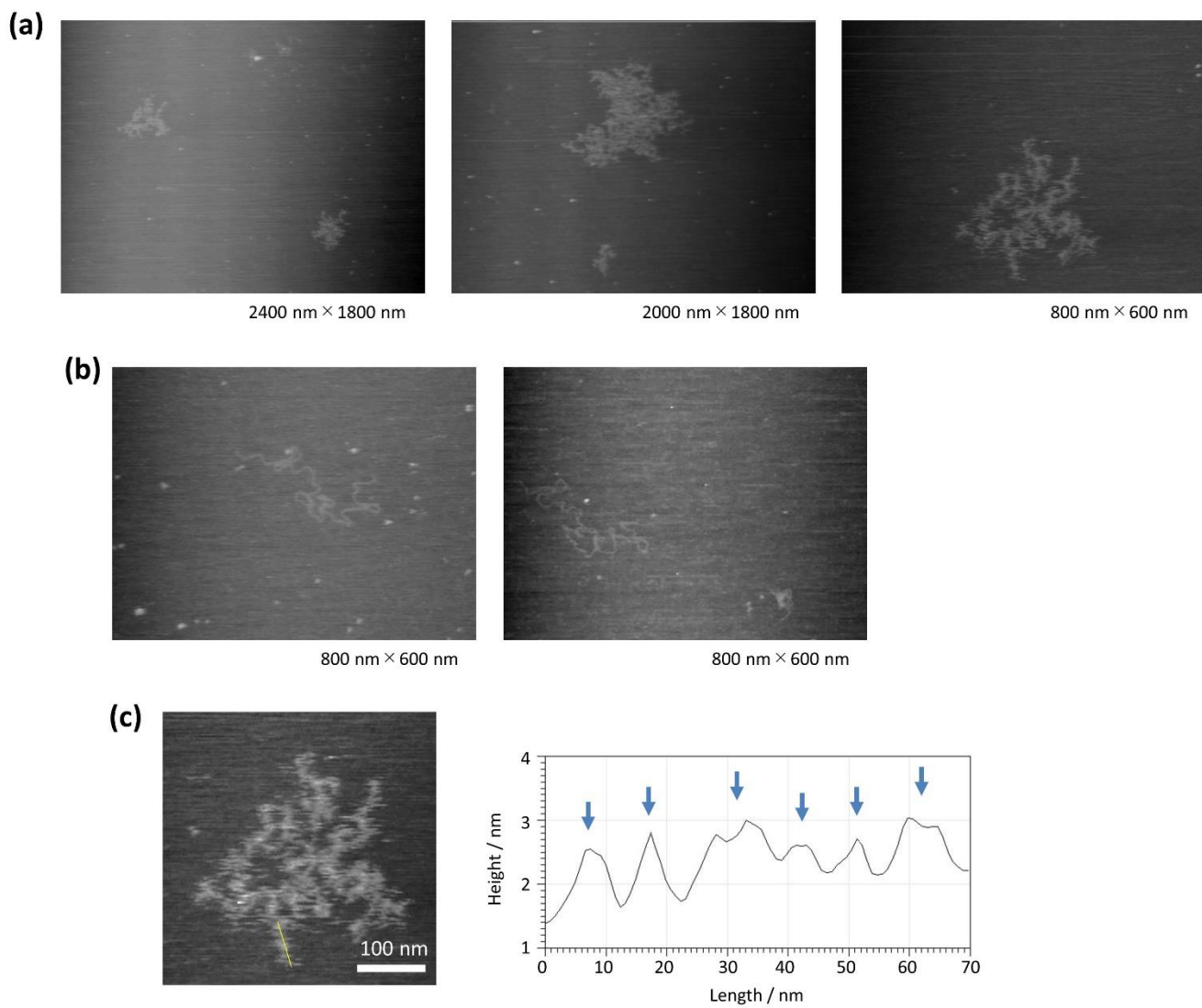
Figure S3. AFM images of a photoresponsive mechanical DNA polymer after UV and VIS irradiation. (a) AFM images of DNA polymers after UV irradiation (shrinked state). (b) AFM images after UV and VIS irradiation (re-relaxed state). (c) Height profile of the line in the image. Successive peaks in the shrinked DNA polymer were detected, which may correspond to the formed hairpins.
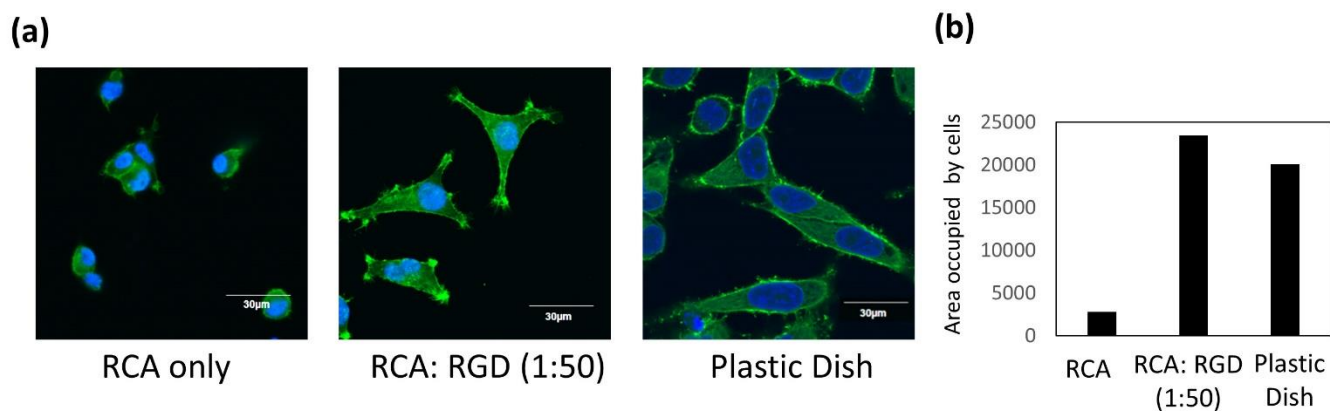
(a) RCA only | RCA: RGD (1:50) | Plastic Dish

(b)

Figure S4. Comparison of cell areas and spreading for different substrates. DNA Polymer coated glass for cell adhesion and spreading. (a) Confocal images of HeLa cells cultured on 3 different substrates (only RCA product, poly RGD (1:50), on cell culture plate). (b) The cell spreading area quantified manually using Image J. 50 cells were analysed in each sample.
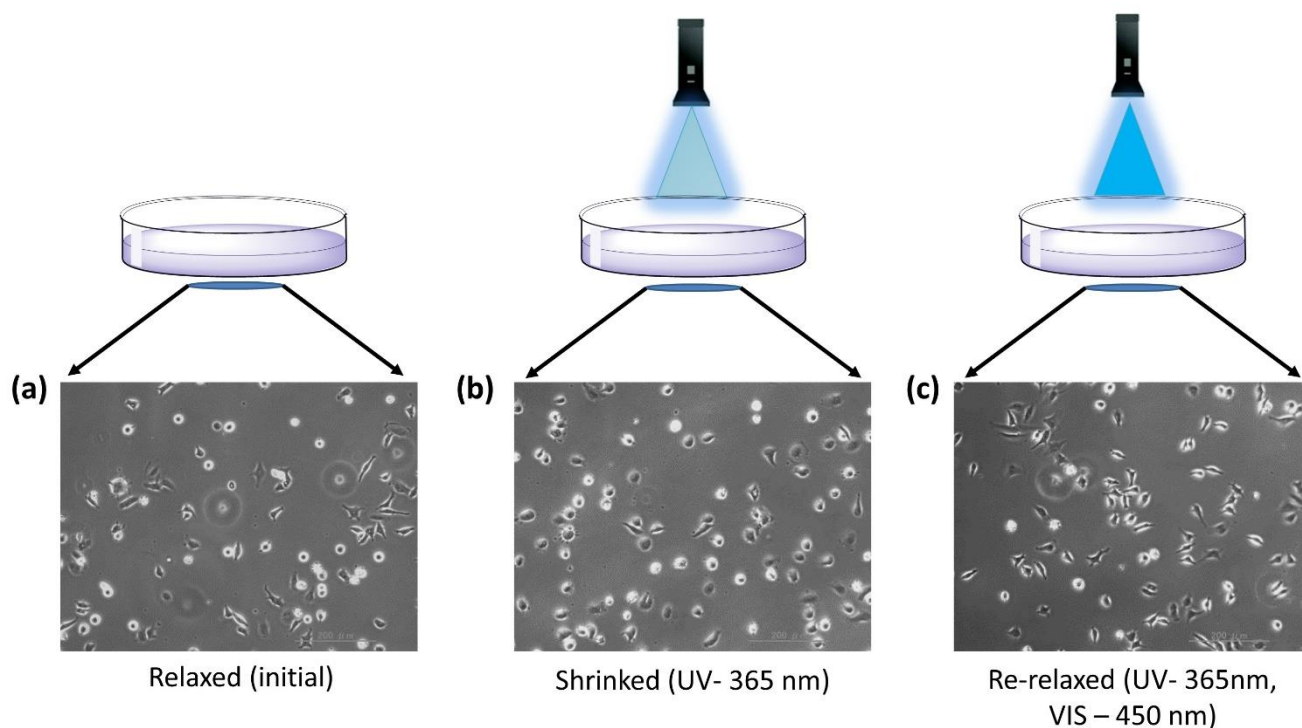

(a) Relaxed (initial) | **(b)** Shrinked (UV- 365 nm) | **(c)** Re-relaxed (UV- 365nm, VIS – 450 nm)

Figure S5. Spatial and Temporal Control of HeLa cell morphology. Phase contrast images of HeLa cells on DNA Polymer coated glass. (a) represents HeLa cells on extended DNA polymer (b) represents HeLa cells on contracted DNA polymer. (c) represents HeLa cells on re-extended DNA polymer. Scale bar: 200 μm.
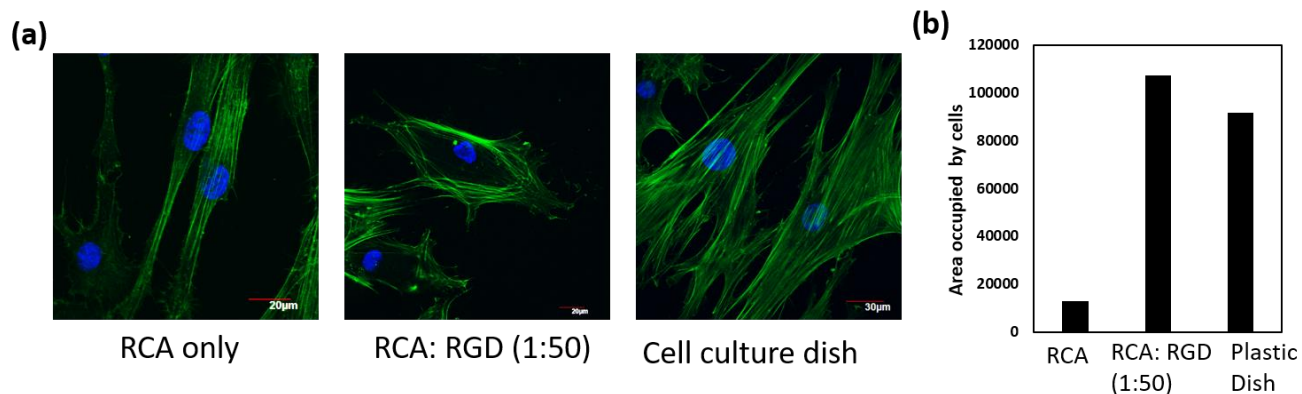
Figure S6. Comparison of cell areas and spreading for different substrates. DNA Polymer coated glass for cell adhesion and spreading. (a) Confocal images of hMSC cells cultured on 3 different substrates (only RCA product, poly RGD (1:50), on cell culture plate). (b) The cell spreading area quantified manually using Image J. 30 cells were analysed in each sample
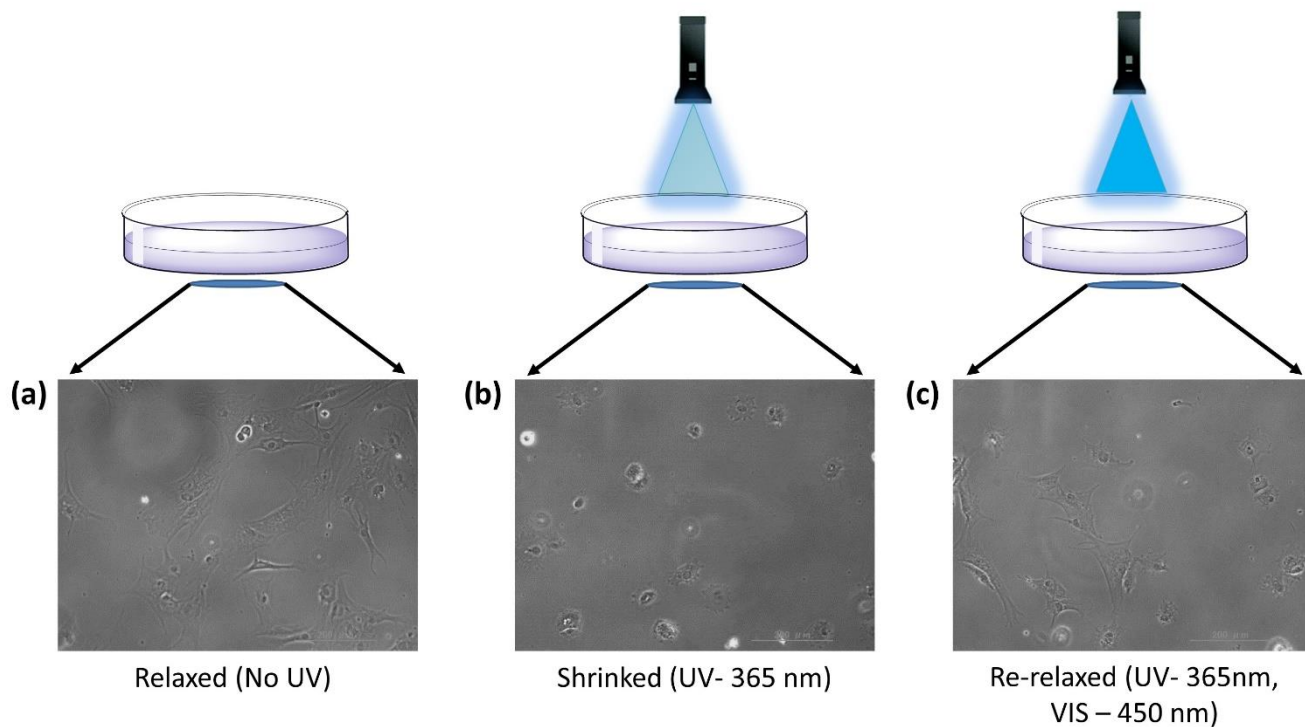

Figure S7. Spatial and temporal control of MSC morphology. Phase contrast images of MSCs on DNA polymer coated glass. (a) represents MSCs on extended DNA polymer. (b) represents ESCs on contracted DNA polymer. (c) represents MSCs on re-extended DNA polymer. Scale bar: 200 μm.
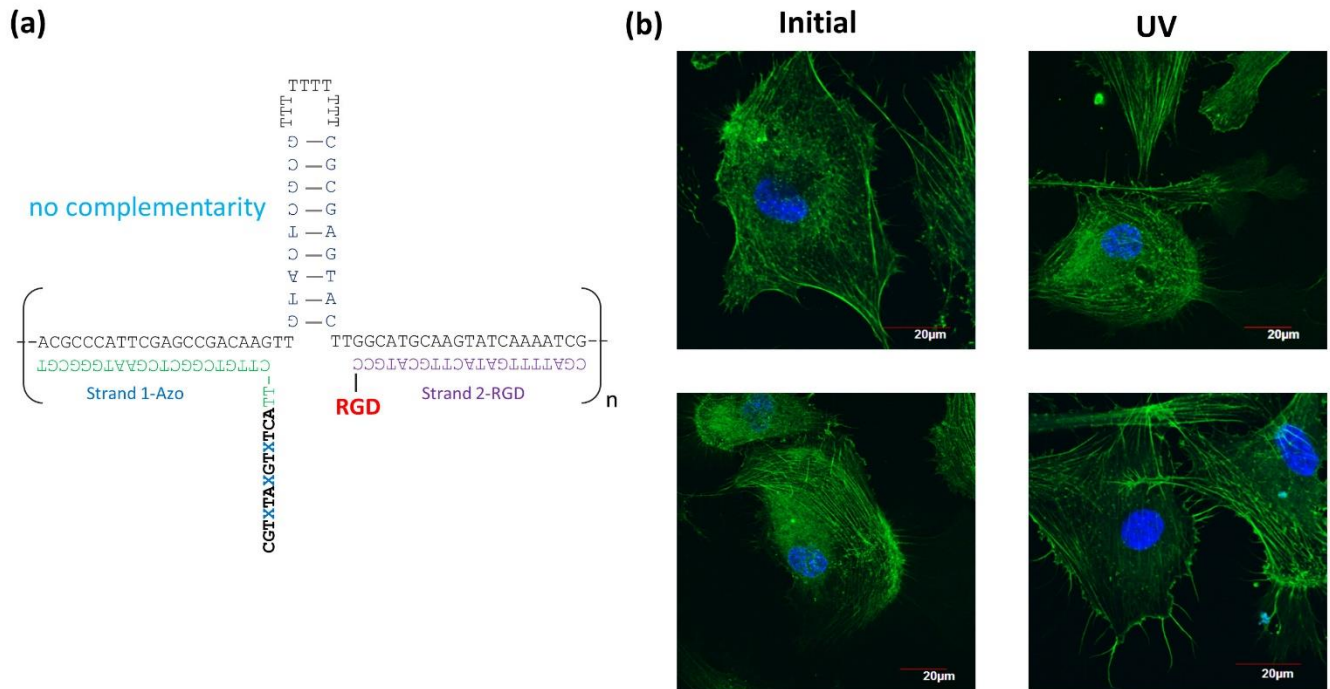
Figure S8. A control experiment to rule out of the possibility that UV light is responsible for the morphology change. A control strand with no complementarity with S1-Azo was chosen for the experiment. (a) Depicts the predicted structure after annealing. (b) hMSCs on initial substrate and after UV irradiation. 30 cells were analyzed for each sample.

Table S1. DNA sequences used in the experiment.

DNA strand	Sequence (5´ to 3´)
Template strand	ACGCCCATTCGAGCCGACAAGTTGAAACTAACGTTTTTTTTTTTCTTAGTATCTTGGCATGCAA GTATCAAAATCG
Template strand (phosphorylated)	(Pho)- ACGCCCATTCGAGCCGACAAGTTGAAACTAACGTTTTTTTTTTTCTTAGTATCTTGGCATGCAA GTATCAAAATCG
Ligation strand	CATAGTTTTAGCTGCGGGTAAGCT
Strand-1-Azo	CGT**X**TA**X**GT**X**TCATTCTTGTCGGCTCGAATGGGCGT (**X**=Azo)
Strand-1-Azo (Dabsyl)	CGT**X**TA**X**GT**X**TCATT(Dabsyl)CTTGTCGGCTCGAATGGGCGT (**X**=Azo)
Strand-2-SH	CGATTTTGATACTTGCATGCC-(SH) (for RGD modification)
Strand-2-FAM	CGATTTTGATACTTGCATGCC-(FAM)

Table S2. Primers used for RT-PCR

GENE	Forward Primer (5´ to 3´)	Reverse Primer(5´ to 3´)
GAPDH	CTGAGCAGACCGGTGTCACATC	GAGGACTTTGGGAACGACTGAG
FAK	GGGCATCATTCAGAAGATAGTG	GTGGGTGGGCGAGTTCAT
Vinculin	TGGTCTAGCAAGGGCAATGA	GGATTCGCTCGCATACCTGT
Paxillin	ATTTGGGGGTCTGCTTCCTG	GACACCGGCTTTCCTGAGAA

References

[1]   R. Deng, L. Tang, Q. Tian, Y. Wang, L. Lin, J. Li, *Angew. Chemie - Int. Ed.* **2014**, *53*, 2389–2393.

[2]   K. Zhang, R. Deng, Y. Sun, L. Zhang, J. Li, *Chem. Sci.* **2017**, *8*, 7098–7105.

[3]   B. Zhao, C. O'Brien, A. P. K. K. K. Mudiyanselage, N. Li, Y. Bagheri, R. Wu, Y. Sun, M. You, *J. Am. Chem. Soc.* **2017**, *139*, 18182–18185.